

Mg²⁺-Fe²⁺ ORDER-DISORDER AND THE THERMODYNAMICS OF THE ORTHO- PYROXENE CRYSTALLINE SOLUTION

SURENDRA K. SAXENA AND SUBRATA GHOSE, *Planetology Branch,
Goddard Space Flight Center, Greenbelt, Maryland 20771.*

ABSTRACT

The distribution of Mg²⁺ and Fe²⁺ between the *M1* and *M2* sites in orthopyroxene (Fe, Mg)₂Si₂O₆ at 500, 600, 700, and 800°C, determined by Mössbauer resonance spectroscopy, can be interpreted in terms of Guggenheim's (1967) "simple mixture" model for the individual sites. The standard free energy change ΔG° for the Fe²⁺-Mg²⁺ exchange between the two sites and the adjustable energy constants *W* for the Fe²⁺-Mg²⁺ mixing on the *M1* and *M2* sites vary linearly with the inverse of the absolute temperature between 600 and 800°C. Fe²⁺-Mg²⁺ mixing at the *M1* site is more non-ideal than that at the *M2* site, both approaching ideality with increasing temperature. "Partial" excess thermodynamic functions of mixing of Mg²⁺-Fe²⁺ on the individual sites are calculated using the "simple mixture" model.

The activity-composition relation in orthopyroxene is derived from the "partial" activities of Mg²⁺ and Fe²⁺ at the two sites at 500, 600, 700, and 800°C. The excess free energy of mixing of the Fe and Mg components in orthopyroxene at various temperatures is expressed as a polynomial in the mole fraction, using Guggenheim's equation with three constants *A*₀, *A*₁, and *A*₂, all of which decrease systematically as the temperature increases from 600 to 800°C.

The orthopyroxene crystalline solution is asymmetric; the asymmetry increases with decreasing temperature. Theoretically orthopyroxene on the Fe-rich side would begin to unmix into two coexisting pyroxenes in the vicinity of 500°C.

INTRODUCTION

Long-range order-disorder phenomenon in alloy phases has been studied extensively. Alloys are characterized, first, by a pattern of sites occupied by atoms irrespective of their chemical nature and, second, by the distribution of the atoms among these sites. This distribution may vary continuously as a function of temperature without a phase transformation. Above a certain critical temperature, the distribution is completely random. With lowering of temperature ordering sets in abruptly, at first increasing rapidly, but becoming complete only as absolute zero is approached.

Long-range order-disorder phenomenon in ferromagnesian silicates, e.g., olivine (Fe, Mg)₂SiO₄, orthopyroxene (Fe, Mg)₂Si₂O₆, cummingtonite (Fe, Mg)₇Si₈O₂₂(OH)₂, etc., differ from that in alloys in several important respects: first, as opposed to alloys, only a certain number of the cations take part in the site exchange, while the silicate framework remains more or less undisturbed; second, usually complete solid solution exists between the Mg and Fe end-members, and third, there may not be any critical temperature above which complete order is attained. A crystalline

solution $(A_xB_{1-x})Z$ may have different cations A and B occupying two different structural sites α and β , where Z represents the silicate framework which does not change compositionally. Following Dienes (1955) and Mueller (1961, 1962), the order-disorder phenomenon can be treated as an ion-exchange reaction:



The order-disorder phenomenon as a function of temperature and chemical composition then can be interpreted in terms of the thermodynamics of homogeneous phase equilibria as developed by Gibbs. Orthopyroxene $(\text{Fe, Mg})_2\text{Si}_2\text{O}_6$, a widely occurring ferromagnesian mineral, provides such a simple case. Here Fe^{2+} and Mg^{2+} can distribute themselves in different amounts between two structural sites $M1$ and $M2$, while rest of the silicate framework remains virtually unchanged. The structure of orthopyroxene consists of infinite single silicate chains held together by infinite octahedral strips. Fe^{2+} and Mg^{2+} ions occur within this octahedral strip, made up of $M1\text{-O}$ and $M2\text{-O}$ octahedra. Since the $\text{Fe}^{2+}\text{-Mg}^{2+}$ exchange between the $M1$ and $M2$ sites takes place within a plane (parallel to the bc plane), only octahedral $M\text{-O}$ bonds are broken. As a result, at high temperatures the exchange process is very rapid and the activation energy is comparatively low. Above 500°C the equilibrium $\text{Fe}^{2+}\text{-Mg}^{2+}$ distribution between the $M1$ and $M2$ sites can be attained in a matter of weeks. The $\text{Mg}^{2+}\text{-Fe}^{2+}$ distribution found in orthopyroxenes from metamorphic, plutonic, and volcanic rocks, as well as meteorites, reflects past thermal history, when temperatures were sufficiently high for $\text{Mg}^{2+}\text{-Fe}^{2+}$ exchange to take place. To be able to interpret the cooling history of such orthopyroxenes on the basis of the $\text{Mg}^{2+}\text{-Fe}^{2+}$ distribution data, we must know the equilibrium $\text{Mg}^{2+}\text{-Fe}^{2+}$ distribution at various temperatures as well as the kinetics of the ordering process.

The first purpose of this paper is to analyze the temperature and compositional dependence of $\text{Mg}^{2+}\text{-Fe}^{2+}$ order-disorder in orthopyroxene thermodynamically. This analysis is based on experimental data on the site occupancy fraction of $\text{Mg}^{2+}\text{-Fe}^{2+}$ at the $M1$ and $M2$ sites in orthopyroxenes of various composition heated at 500, 600, 700, and 800°C , and the use of solution models to explain the mixing of Fe^{2+} and Mg^{2+} on the individual sites. The study of the solution behavior at the sites makes it possible to obtain a thermodynamic model of the orthopyroxene crystalline solution as a whole. Using such a model, thermodynamic functions of mixing of the cations Fe^{2+} and Mg^{2+} in the crystal can be calculated. These functions of mixing, namely, free energy, enthalpy, and entropy, are comparable in magnitude to those found by calorimetric experiments on the solution of MgSiO_3 and FeSiO_3 .

PREVIOUS WORK

The thermodynamic significance of the distribution of cations among co-existing mineral phases was initially discussed by Ramberg (1944, 1952). Such heterogeneous distributions, now being studied intensively by many petrologists, are related to internal reactions within individual mineral phases. Experimental evidence of homogeneous reactions within ferromagnesian silicates such as cummingtonites and orthopyroxenes were presented by Ghose and Hellner (1959) and Ghose (1961, 1965). These results encouraged thermodynamic treatment of the intracrystalline distribution of cations on nonequivalent sites and of the heterogeneous equilibria, *i.e.*, the distribution of cations between two or more coexisting phases by Mueller (1961, 1962, 1967, 1969), Matsui and Banno (1965), Banno and Matsui (1966, 1967), Grover and Orville (1969), and Thompson (1969).

Orthopyroxenes have been studied extensively by X-ray diffraction as well as by the Mössbauer resonance technique and the problem of intracrystalline distribution over *M1* and *M2* sites is well defined. By X-ray diffraction Ghose (1965) found that Fe^{2+} is preferred strongly at the *M2* site and Mg^{2+} at the *M1* site. He also predicted the temperature dependence of the site occupancies, which was confirmed later by Evans, Ghose, and Hafner (1967) and Ghose and Hafner (1967) using the Mössbauer resonance technique. The Mössbauer technique has been used also by Bancroft, Burns, and Howie (1967), Marzolf, Dehn, and Salmon (1967), and Dundon and Walter (1967) to determine Mg^{2+} - Fe^{2+} distribution in plutonic and volcanic, synthetic and meteoritic orthopyroxenes respectively. Virgo and Hafner (1969) determined the kinetics of Mg^{2+} - Fe^{2+} order-disorder in an intermediate orthopyroxene ($X_{\text{Fe}}^{\text{Opx}} = 0.575$) and the Mg^{2+} - Fe^{2+} distribution isotherm at 1000°C. Ghose and Hafner (1967) and Virgo and Hafner (1969) presented the order-disorder relations or the intra-crystalline distribution by an ion-exchange equation for Fe^{2+} and Mg^{2+} between *M1* and *M2* sites.

From these investigations (principally Virgo and Hafner, 1969), it is now generally established that in orthopyroxene (1) the ion-exchange takes place between 480°C to 1000°C, (2) the activation energies required for ordering and disordering are relatively low, and (3) the ion-exchange is a rapid process. Ghose and Hafner (1967) and Virgo and Hafner (1969, 1970) discussed the mixing of Mg^{2+} - Fe^{2+} at the *M1* and *M2* sites by referring to an ideal solution model. This assumption was found to be valid in the case of Mg^{2+} - Fe^{2+} distribution isotherm at 1000°C for $\text{Fe}^{2+}/(\text{Fe}^{2+} + \text{Mg}^{2+})$ in orthopyroxene $X_{\text{Fe}}^{\text{Opx}} < 0.70$ determined by Virgo and Hafner (1969). They have also determined Mg^{2+} - Fe^{2+} distribution between *M1* and *M2* sites in one orthopyroxene, ($X_{\text{Fe}}^{\text{Opx}} = 0.575$) at 500, 600,

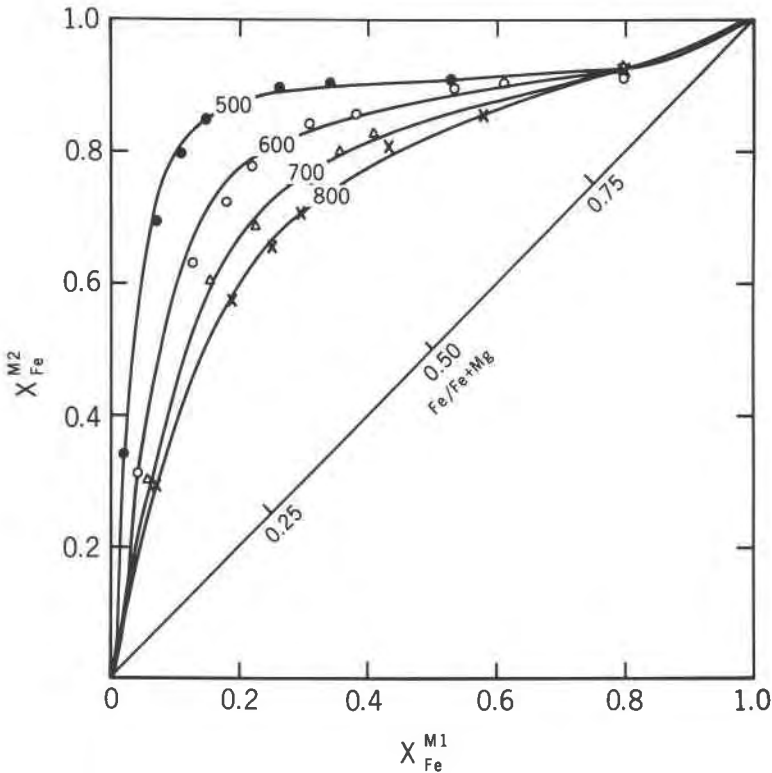


FIG. 1. Distribution of Fe^{2+} and Mg^{2+} between $M1$ and $M2$ sites in orthopyroxenes heated at 500, 600, 700, and 800°C.

700, 800, and 1000°C. On the basis of these data on one sample, they extrapolated Mg^{2+} - Fe^{2+} distribution isotherms for 500, 600, 700, and 800°C assuming the ideal solution model for the individual sites to be valid down to 500°C. Virgo and Hafner (1970) also determined Mg^{2+} - Fe^{2+} distribution in a large number of metamorphic and plutonic orthopyroxenes. These distribution data show a small range of scatter, indicating that these orthopyroxenes were presumably quenched around 500°C. However, these data points straddle the hypothetical distribution isotherms from 500 to 1000°C based on the ideal solution model (Virgo and Hafner, 1970, Figure 1). Obviously the mixing on the $M1$ and $M2$ sites is not ideal at lower temperatures. Saxena and Ghose (1970) used the regular solution model to interpret these data and the success of this approach prompted the determination of complete Mg^{2+} - Fe^{2+} distribution isotherms at various temperatures in orthopyroxene.

Activity-composition relation in pyroxenes at 1200°C has been discussed by Nafziger and Muan (1967) and Kitayama and Katsura (1968).

THERMODYNAMICS

The following abbreviations and symbols are used:

Opx, orthopyroxene

$X_{\text{Fe}}^{\text{Cpx}}$, mole fraction $\text{Fe}^{2+}/(\text{Fe}^{2+} + \text{Mg}^{2+})$ in the crystal as a whole

X_{Fe}^{M1} , site occupancy factor or the atomic ratio $\text{Fe}^{2+}/(\text{Fe}^{2+} + \text{Mg}^{2+})$ on site $M1$ and similarly X_{Fe}^{M2}

R , gas constant; T , absolute temperature

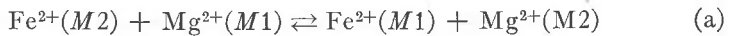
K , equilibrium constant; K_D , distribution coefficient

G_a , free energy of the reaction (a)

$W^{M1(\text{or } M2)}$, an adjustable constant referred to the site $M1$ (or $M2$)

$f_{\text{Fe}}^{M1(\text{or } M2)}$, partial activity coefficient for $M1$ (or $M2$)

The ion-exchange between the $M1$ and $M2$ sites in orthopyroxene, $(\text{Mg,Fe})_2\text{Si}_2\text{O}_6$ can be written as:



The equilibrium constant for the above reaction is

$$K_a = \frac{X_{\text{Fe}}^{M1}(1 - X_{\text{Fe}}^{M2}) f_{\text{Fe}}^{M1} f_{\text{Mg}}^{M2}}{(1 - X_{\text{Fe}}^{M1})X_{\text{Fe}}^{M2} f_{\text{Mg}}^{M1} f_{\text{Fe}}^{M2}} \quad (1)$$

and the free energy change is $\Delta G_a^0 = -RT \ln K_a$.

As indicated by Thompson (1969) and Mueller, Ghose and Saxena (1970), it is not possible to define chemical potential of a cation on different sites in a crystal. Therefore f is called the partial activity coefficient here. Equation (1) is written in analogy with the heterogeneous equilibrium distribution of a species between two non-ideal mixtures. $M1$ and $M2$ sites are treated as two interpenetrating subsystems, and the thermodynamic relations established for macroscopic systems are used directly. The physical significance of the partial thermodynamic functions of mixing with respect to the sites is not yet clear; but by virtue of the definiteness of the site occupancy factors or the mole fractions at each site, these partial quantities are also definite.

We define a factor W such that

$$\ln f_{\text{Fe}}^{M1} = \frac{W^{M1}}{RT} (1 - X_{\text{Fe}}^{M1})^2 \quad (2)$$

This is analogous to the equation (818.6) derived by Fowler and Guggenheim (1939) in connection with the "strictly regular" solution model. This

crude treatment implies a completely random distribution of the cations within a phase and the change of entropy on mixing is the same as for the ideal solution. The factor W referred to as "the interchange energy" is independent of temperature in Guggenheim's (1952) original model. In the present paper W is used as an adjustable constant to fit the experimental data, which is not necessarily independent of temperature. This treatment is consistent with Guggenheim's (1967) latest ideas where he calls such solutions 'simple mixtures.'

Substituting the values of f from (2) in (1) for K_a we obtain an expression as used by Mueller (1964) or to facilitate computation in a logarithmic form as used by Saxena (1969)

$$\ln K_D - \ln K_a = \frac{W^{M_2}}{RT} (1 - 2X_{\text{Fe}}^{M_2}) - \frac{W^{M_1}}{RT} (1 - 2X_{\text{Fe}}^{M_1}) \quad (3)$$

where K_D is the distribution coefficient,

$$\frac{X_{\text{Fe}}^{M_1} (1 - X_{\text{Fe}}^{M_2})}{X_{\text{Fe}}^{M_2} (1 - X_{\text{Fe}}^{M_1})}$$

If the intra-crystalline distribution data are in close agreement with (3), the 'partial' excess thermodynamic functions of mixing on individual sites can be evaluated, which are analogous to those of the macro-system. The 'partial' excess function of mixing for M_1 , for example, are

$$G^E = X_{\text{Fe}}^{M_1} (1 - X_{\text{Fe}}^{M_1}) W^{M_1}; \quad W^{M_1} = W(T, P) \quad (4)$$

$$-S^E = X_{\text{Fe}}^{M_1} (1 - X_{\text{Fe}}^{M_1}) \frac{\partial W^{M_1}}{\partial T} \quad (5)$$

$$H^E = X_{\text{Fe}}^{M_1} (1 - X_{\text{Fe}}^{M_1}) W^{M_1} - T \frac{\partial W^{M_1}}{\partial T} \quad (6)$$

EXPERIMENTAL

Chemical Analysis of the Samples. All pyroxene samples used as starting material were separated from various metamorphic rocks. Separates were hand picked under the microscope to achieve a purity of 98 percent or better. Chemical analyses of these samples, eight of which are new, are listed in Table 1. The microprobe analyses were made by using natural pyroxene standards and the data were processed using the Bence and Albee (1968) correction method. The wet chemical analysis of the sample XYZ is taken from Ramberg and DeVore (1951).

Microscopic examination of the pyroxenes did not show zoning or any significant amount of unmixing. Several grains from each sample were analyzed by the microprobe to check for homogeneity in chemical composition, particularly for iron and magnesium. The

TABLE 1. CHEMICAL ANALYSES OF ORTHOPYROXENES

Ref. No.	1	2	3	4	5	6	7	8	9
SiO ₂	56.51	51.23	52.98	51.75	51.40	51.05	49.64	48.39	47.5
Al ₂ O ₃	0.00	1.59	0.03	0.72	0.08	0.04	0.06	0.33	1.20
TiO ₂	0.02	0.06	0.12	0.21	0.18	0.15	0.22	0.30	0.28
FeO ^a	11.76	23.46	27.80	30.11	33.80	35.13	40.73	41.80	46.00
MnO	1.77	0.09	0.98	0.84	0.80	0.78	0.84	1.00	0.05
MgO	29.49	21.13	18.46	16.71	13.51	11.95	8.79	7.28	3.99
CaO	0.28	0.48	0.49	0.64	0.62	0.52	0.74	0.86	0.92
Na ₂ O	0.02	0.00	0.05	0.08	0.11	0.15	0.08	0.18	n.d.
K ₂ O	0.00	0.00	0.01	0.05	0.02	0.02	0.02	0.03	n.d.
Total	99.85	98.04	100.92	101.11	100.52	99.79	101.12	100.17	99.95
Fe/(Fe+Mg)	0.181	0.381	0.455	0.500	0.580	0.620	0.720	0.760	0.86

^a FeO is total iron calculated as FeO. n.d. = not determined.

1 to 8. New x-ray electron probe analyses. No. 9 wet chemical analysis.

1. Sample No. 274, Butler (1969).

2. Sample No. T3/66, Saxena (1968).

3. Sample No. 277, Butler (1969).

4. Sample No. 10, Arendalite, collected by Saxena from the type locality in Norway.

5. Sample No. 264, Butler (1969).

6. Sample No. 278, Butler (1969).

7. Sample No. 207, Butler (1969).

8. Sample No. 10/68, charnockite from Varberg, collected by Saxena.

9. Sample No. XYZ, Ramberg and DeVore (1951).

grain to grain compositional variation was less than one weight percent of FeO or MgO. Sample 7, however, was found to be somewhat heterogeneous, where FeO varied within 2 percent.

Heating Experiments. About 50 to 100 mg. of the orthopyroxene sample was loaded in a gold capsule and heated in internally heated cold-seal pressure vessels under an argon pressure of 0.5 to 1.5 kbar. The pressure was measured using a Bourdon tube gauge. The gold capsules were left open so that argon could pass freely through the capsule during heating. The temperature was measured by using sheathed chromel-alumel thermocouple calibrated at one atmosphere at the melting point (800.5°C) of NaCl. It was controlled to within $\pm 3^\circ\text{C}$ and the accuracy in measurement is better than $\pm 10^\circ\text{C}$. The temperature was monitored continuously on a Honeywell multi-channel potentiometer with semi-continuous print-out.

The duration of the heating runs required for a close approach to the Mg²⁺-Fe²⁺ exchange equilibrium was estimated on the basis of the kinetic experiments on orthopyroxenes (Virgo and Hafner, 1969). The orthopyroxene samples were heated at 500° and 600°C for periods of three and two weeks respectively and at 700 and 800°C for a period of one week. In all cases, the heating runs were much longer than that required for equilibration (Virgo and Hafner, 1969, Figure 2). The heated samples were quenched by blowing cold air on the pressure vessel. The temperature dropped to below 300°C within seconds. The orthopyroxene grains were removed from the gold capsules and examined under the microscope for possible oxidation.

Mössbauer Resonance Experiments. The Mössbauer resonance spectrometer was of the constant acceleration type. The Doppler shift between the moving source and the stationary absorber was applied by means of an electromechanical drive of the Kankeleit type. 50 mCi ⁵⁷Co diffused into copper foil was used as the source for the 14.4 keV gamma rays.

The absorbers were prepared by mixing 50–100 mg of the finely powdered orthopyroxene with 500 mg of lucite and pressing into a 1" diameter disc. The thickness amounted to about 3–5 mg of Fe per cm². All spectra were recorded with the absorbers cooled to liquid nitrogen temperature. For this purpose, a vertical stainless steel cryostat (built by Austin Science Associates) was used so that horizontal transmission geometry could be maintained. The temperature achieved this way must be in the vicinity of 77°K, though an exact measurement of the absorber temperature has not been made. Compared to the room temperature spectra, at liquid nitrogen temperature, the quadrupole splitting of the outer doublet *A1-B1* due to ⁵⁷Fe at *M1* increases considerably, while the splitting of the inner doublet *A2-B2* due to ⁵⁷Fe at *M2* remains virtually the same (Shenoy, Kalvius, and Hafner, 1969). This results in a considerable improvement in the resolution of the spectra and hence in the calculation of area ratios and site occupancy factors. A 0.004" aluminum foil was placed between the source and the absorber to filter the copper X-rays. The transmitted gamma ray pulses were counted by means of a proportional counter filled with 90 percent Krypton and 10 percent methane at 1 atm. The multi-channel analyzer was operated in the time mode. The pulses were accumulated in 512 channels. In general about 2.5 × 10⁶ counts per channel were recorded for each spectrum. Average counting time was about 20 hours. The spectrometer has been calibrated against a standard Fe-foil of 99.999 percent purity provided by J. J. Spijkermann of the National Bureau of Standards. Only the inner four lines were used for calibration. The measured line widths of the iron lines are: inner pair 0.26 mm/sec., outer pair 0.28 mm/sec. The calibration spectra were taken every week. No detectable drift in the spectrometer has been found.

A least squares program was used on the IBM 360/75 computer to fit Lorentzian curves to the two overlapping doublets of the orthopyroxene spectra without any constraints. The number of variable parameters was 13, *i.e.*, 3 per absorption peak and 1 for the off-resonant baseline. The chi-square values ranged between 150–300. The calculated standard errors in the line-widths at half-intensity (half-widths) were consistently much higher than those for the line-intensities. However, the calculated area ratios fall on a smooth curve when plotted against the Fe/(Fe+Mg) ratio of the total crystal. This indicates a high level of consistency in our results. Absolute limits to the calculated peak areas cannot be ascertained. Incidentally, it was found that for lower counting statistics (1 × 10⁶ counts per channel or less) the calculated errors for half-widths are considerably larger and area ratio vs Fe/(Fe+Mg) ratio of the crystal yields a plot with much greater scatter.

The peak nomenclature is as follows: lower velocity peaks, *A1* and *A2*; higher velocity peaks *B2* and *B1*. The inner pair, *A2-B2* from ⁵⁷Fe at the *M2* site is always more intense than the outer pair, *A1-B1* from ⁵⁷Fe at the *M1* site. This site assignment is unambiguous and is based on the known preference of Fe for the highly distorted *M2* site (Ghose, 1965). The site occupancy factors were calculated assuming the recoilless fraction at the *M1* and *M2* sites to be equal. The site occupancy factor for *M1*, for example, is given by

$$\frac{[I_{A1} \times \Gamma_{A1} + I_{B1} \times \Gamma_{B1}]}{[I_{A1} \times \Gamma_{A1} + I_{A2} \times \Gamma_{A2} + I_{B1} \times \Gamma_{B1} + I_{B2} \times \Gamma_{B2}]} \times 2Fe^{2+}/(Fe^{2+} + Mg^{2+}),$$

where *I* is the intensity and Γ is the half width of a Mössbauer resonance peak. Calculated this way, the site occupancy factors for *M1* and *M2* are the mole fractions Fe²⁺/(Fe²⁺ + Mg²⁺) at each site.

RESULTS

Table 2 lists the results of the Mössbauer experiments on the heated orthopyroxenes. Figure 1 shows the distribution of Fe²⁺ and Mg²⁺ be-

TABLE 2. LINE WIDTHS AND INTENSITIES OF THE MÖSSBAUER SPECTRA AND THE CALCULATED SITE OCCUPANCY FACTORS AT THE $M1$ AND $M2$ SITES OF ORTHOPYROXENES, $(\text{Fe, Mg})_2\text{Si}_2\text{O}_6$

Ref. No.	$X_{\text{Fe}}^{\text{Opx}}$	Line widths (full width at half height) mm/sec				Intensities referred to $I (A_1 + A_2 + B_1 + B_2) = 1.0$				Fe ²⁺ site occupancy factors	
		A1	A2	B2	B1	A1	A2	B2	B1	X_{Fe}^{M1}	X_{Fe}^{M2}
500°C											
1.	0.181	.2583	.3514	.2588	.2725	.0243	.5305	.4036	.0415	0.021	0.341
2.	0.381	.2612	.3441	.3054	.3167	.0606	.5207	.3750	.0435	0.070	0.692
3.	0.455	.2915	.3059	.2650	.3457	.0523	.4951	.3939	0.585	0.111	0.799
4.	0.500	.3244	.3366	.3294	.3380	.0803	.4551	.3942	0.703	0.150	0.850
5.	0.580	.2454	.3013	.2825	.3014	.1143	.4268	.3355	.1232	0.262	0.897
6.	0.620	.2754	.3390	.2917	.3413	.1273	.4057	.3175	.1495	0.337	0.902
7.	0.720	.2798	.2982	.2867	.3065	.1767	.3411	.2903	.1918	0.533	0.907
600°C											
1.	0.181	.2131	.3462	.2693	.3461	.0684	.5128	.3469	.0718	0.046	0.316
2.	0.381	.3972	.3911	.3818	.4025	.0785	.4822	.3545	.0848	0.129	0.632
3.	0.455	.2895	.3462	.3106	.3166	.1031	.4368	.3450	.1151	0.186	0.726
4.	0.500	.2677	.3582	.3169	.3128	.1169	.4284	.3248	.1298	0.219	0.781
5.	0.580	.2686	.3408	.3079	.3356	.1327	.4061	.3120	.1491	0.310	0.849
6.	0.620	.2920	.3121	.2832	.2866	.1460	.3839	.3001	.1698	0.382	0.857
7.	0.720	.2879	.3093	.2905	.3000	.1771	.3584	.2576	.2069	0.545	0.895
8.	0.760	.3308	.3255	.3116	.3001	.1999	.3346	.2586	.2069	0.613	0.905
9.	0.860	.2915	.3075	.3154	.3169	.2234	.2910	.2403	.2453	0.797	0.922
700°C											
1.	0.181	.3621	.3695	.3543	.2842	.0943	.4549	.3677	.0830	0.059	0.303
2.	0.381	.3580	.4020	.3418	.4112	.0946	.4602	.3387	.1065	0.156	0.605
3.	0.455	.3478	.2913	.3076	.2992	.1243	.4132	.3552	.1072	0.225	0.685
5.	0.580	.2958	.2809	.2929	.2990	.1416	.3853	.3127	.1604	0.360	0.800
6.	0.620	.3411	.3343	.3400	.3173	.1583	.3604	.3029	.1783	0.410	0.829
9.	0.860	.2838	.3133	.2990	.2951	.2182	.2893	.2370	.2554	0.790	0.929
800°C											
1.	0.181	.2853	.2815	.2904	.2443	.1031	.4402	.3576	.0989	0.069	0.293
2.	0.381	.3446	.3602	.3323	.3645	.1228	.4421	.3148	.1202	0.187	0.575
3.	0.455	.3268	.3347	.3387	.3727	.1296	.3987	.3317	.1398	0.252	0.657
4.	0.500	.3546	.3509	.3270	.3546	.1382	.3888	.3212	.1517	0.298	0.701
6.	0.620	.2780	.3084	.2984	.2981	.1642	.3504	.2920	.1933	0.429	0.811
7.	0.720	.3026	.2862	.3009	.3019	.1884	.3334	.2716	.2066	0.579	0.860
9.	0.860	.2891	.3128	.3060	.2992	.2206	.2903	.2351	.2539	0.794	0.926

tween $M1$ and $M2$ sites at 500, 600, 700, and 800°C. The curves represent least squares fit of the data to equation (3). The data for K_a , W^{M1} , W^{M2} and ΔG_a^0 for the four Mg-Fe distribution isotherms are listed in Table 3. W^{M1} and W^{M2} are plotted against $1/T$ in Figure 2.

TABLE 3. THERMODYNAMIC PARAMETERS OF Fe^{2+} - Mg^{2+} ION-EXCHANGE BETWEEN $M1$ AND $M2$ SITES IN ORTHOPYROXENE, $(\text{Fe}, \text{Mg})_2\text{Si}_2\text{O}_6$ ACCORDING TO EQUATION (3)

T°C	K	Cal/mole		
		W^{M1}	W^{M2}	ΔG_a°
500	0.175	2610	1174	2678
600	0.277	2390	1577	2233
700	0.273	1916	1215	2509
800	0.289	1641	1057	2646

Note: The true intrinsic errors are unknown. Estimated error in the site occupancy fractions is ± 1 percent, as determined from replicate analysis of the same sample. This error leads to ± 5 percent error in W^{M2} , ± 2.0 percent in W^{M1} and ± 7 percent in K_a and ΔG_a° . The estimated error in site occupancy fractions does not include the ± 2 percent analytical errors in determining the bulk composition of the orthopyroxene. Such errors, however, shift the distribution point diagonally. Therefore, the total error in the site occupancies fractions in the 700 and 800°C isotherms and in the middle parts of the 500 and 600°C isotherms will not vary greatly from ± 1 percent.

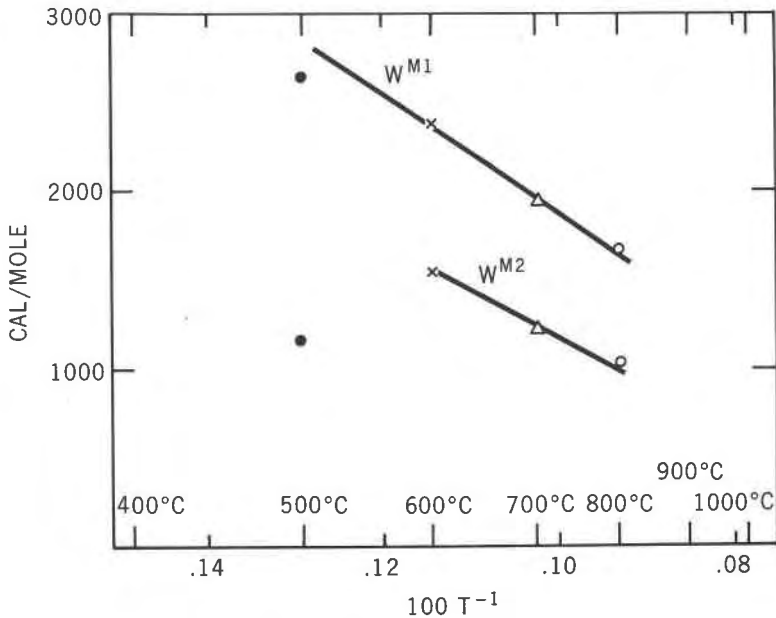


FIG. 2. Variation of W^{M1} and W^{M2} as a function of inverse of absolute temperature.

DISCUSSION

Site Occupancy Factors. For calculating the site occupancy factors X_{Fe}^{M1} and X_{Fe}^{M2} , cations such as Al^{3+} , Ti^{4+} , Mn^{2+} , and Ca^{2+} present in low concentration were not considered, since there is no unambiguous way of assigning these cations to either $M1$ or to $M2$ sites. Ca^{2+} could be restricted to the $M2$ site, but the usual occurrence of microscopic or sub-microscopic exsolution lamellae of calcium-rich pyroxene makes this procedure dubious. Distribution of Mn^{2+} between $M2$ and $M1$ (with a preference for $M2$) is not known. Likewise, Al^{3+} could be present not only in the octahedral $M1$ and $M2$ sites, but also in the $T1$ and $T2$ tetrahedral sites.

In six of the nine samples used, the total of the ions Al^{3+} , Ti^{4+} , Mn^{2+} , and Ca^{2+} was less than 4 percent of the total of Fe^{2+} and Mg^{2+} . Further, as these ions are distributed between $M1$ and $M2$, and, in the case of Al^{3+} and Ti^{4+} , among $M1$, $M2$, $T1$ and $T2$, they are not likely to affect the use of a binary solution model significantly. The influence of these additional components can only be evaluated when the present results are compared with those on pure synthetic Fe^{2+} - Mg^{2+} pyroxenes.

Distribution of Fe^{2+} and Mg^{2+} . The deviation of the solution behavior at each site from the ideal solution model is shown in Figure 3, where $\ln K_D$ is plotted against $X_{\text{Fe}}^{\text{Opx}}$. If the mixing is ideal on both sites, the curves drawn in this figure would be straight lines parallel to the abscissa. Virgo and Hafner (1970) noted the non-ideal behavior at the sites also and discussed the isotherms as being ideal in the Mg-rich part and non-ideal in the Fe-rich part. From the present results it is obvious that a non-ideal model is needed, which is compatible with the entire set of isotherms.

The isotherm at 500°C in Figure 1 is very similar to the curve for the Mg^{2+} - Fe^{2+} distribution data from metamorphic orthopyroxenes (Saxena and Ghose, 1970). The free energies of ion exchange reaction, (a), do not change significantly with change in temperature (Table 3). These values are less than those determined by Virgo and Hafner (1969), since the non-ideality effect on the sites has been taken into account. Note that the ΔG_a^0 at 500°C does not differ appreciably from the values at other temperatures as it did in Virgo and Hafner's (1969) work.

All the isotherms shown in Figure 1 cross at about $X_{\text{Fe}}^{\text{Opx}} = 0.86$ (sample 9). The Mg- Fe^{2+} distribution data for sample 9 at different temperatures are very similar. This means that there is little change in the site occupancy factors X_{Fe}^{M1} and X_{Fe}^{M2} in the temperature range of 500 to 800°C for this sample. Although small changes in X_{Fe}^{M1} and X_{Fe}^{M2} with temperature in this compositional range cannot be determined reliably with the

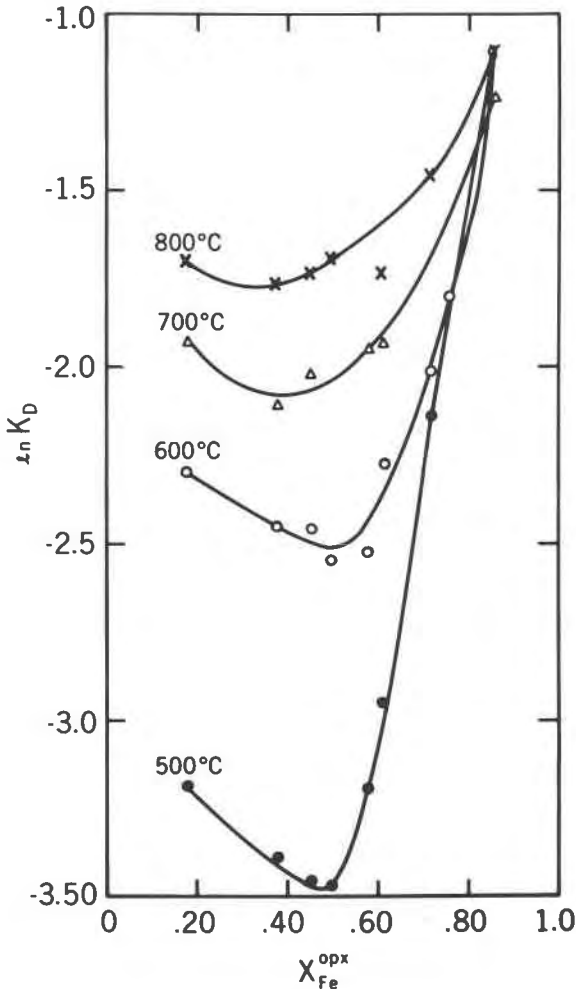


FIG. 3. The compositional $[\text{Fe}^{2+}/(\text{Fe}^{2+} + \text{Mg}^{2+})]$ dependence of natural log of the distribution coefficient ($\ln K_D$) for Mg^{2+} - Fe^{2+} distribution between $M1$ and $M2$ sites. For ideal mixing K_D should be constant for all orthopyroxene compositions.

present experimental technique, the fact that the isotherms for 500°C crosses the isotherm for 800°C may be meaningful on the basis of the consistency of the entire distribution model. Such crossover of distribution isotherms is not unusual, when one or both of the coexisting phases are non-ideal solutions (Saxena, 1969). However, the discussion of this aspect should be postponed until more experimental data in this composition range are available.

Mixing of Fe^{2+} and Mg^{2+} on the $M1$ and $M2$ sites between 500°C and 1000°C . Figure 2 shows that the W^{M1} and W^{M2} values vary linearly with the inverse of absolute temperature in the range 600°C to 800°C . For W^{M1} and W^{M2} the linear relations can be approximated by:

$$\ln W^{M1} = 20.0978 - 1.8203 \ln T \quad (7a)$$

$$\ln W^{M2} = 20.3592 - 1.9220 \ln T \quad (7b)$$

The decrease in W with increasing temperature indicates that the mixing of Mg^{2+} and Fe^{2+} on both the sites approaches ideality with increasing temperature. Using equations (4, 5, 6) the partial excess free energy of mixing, partial excess entropy of mixing and partial excess heat of mixing have been computed and plotted against X^{M1} and X^{M2} in Figure 4.

A linear extrapolation of the W values towards 1000°C shows that the mixing of Fe^{2+} - Mg^{2+} on both sites would be close to ideal at that temperature. This is consistent with the site occupancy data at 1000°C obtained by Virgo and Hafner (1969), who found that the isotherm is ideal for most of the compositional range.

In view of the consistency of the data between 600 to 1000°C , the W values at 500°C appear doubtful. The site occupancy of Fe^{2+} at $M1$ in Mg -rich samples at 500°C is very low and hence cannot be determined very accurately. Even an one percent error in the determination of the site occupancies for Mg -rich samples at 500°C affects the W values significantly.

ACTIVITY-COMPOSITION RELATION

The partial activity coefficient of the Fe component with reference to a site in the orthopyroxene $(\text{Mg}, \text{Fe})_2\text{Si}_2\text{O}_6$ crystalline phase is defined as

$$\ln f_{\text{Fe}}^{M1} = \frac{W^{M1}}{RT} (1 - X_{\text{Fe}}^{M1})^2 \quad (8)$$

where f_{Fe}^{M1} is the partial activity coefficient, W_{Fe}^{M1} an adjustable energy constant, and X_{Fe}^{M1} the atomic fraction $\text{Fe}^{2+}/(\text{Fe}^{2+} + \text{Mg}^{2+})$ on the $M1$ site. The partial activity of Fe^{2+} on the $M1$ site is given by

$$a_{\text{Fe}}^{M1} = f_{\text{Fe}}^{M1} X_{\text{Fe}}^{M1} \quad (9)$$

Similarly for the $M2$ site,

$$a_{\text{Fe}}^{M2} = f_{\text{Fe}}^{M2} X_{\text{Fe}}^{M2} \quad (10)$$

We need a simple model of the macroscopic system, which permits the derivation of the activity of the Fe component in a crystalline orthopyroxene, $(\text{Mg}, \text{Fe})\text{SiO}_3$ phase from the partial activities of the com-

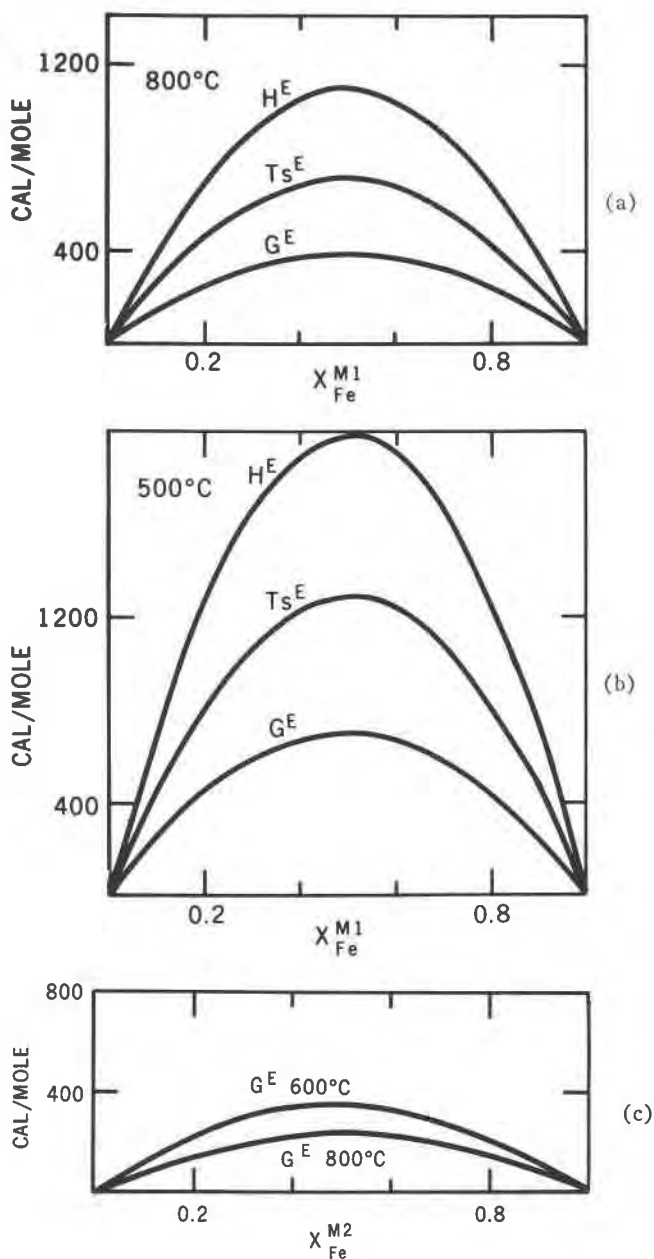


FIG. 4. a and b. Partial thermodynamic functions of mixing—free energy, enthalpy and entropy for the $M1$ site at 500 and 800°C. c. Partial excess free energy of mixing for the $M2$ site at 600 and 800°C. Partial excess heat of mixing is not significantly different from free energy and excess entropy is small.

ponent on individual sites $M1$ and $M2$. On the basis of statistical thermodynamics, such a model is:

$$a_{\text{Fe}}^{\text{Opx}} = (a_{\text{Fe}}^{M1} a_{\text{Fe}}^{M2})^{1/2} \quad (11)$$

Mueller (1962) used such a relation while discussing a solution model for cummingtonite. Banno and Matsui (1967) and Thompson (1970) have also used such a relationship.

Figures 5 and 6 show the plots of partial activity of Fe^{2+} against mole fraction $\text{Fe}^{2+}/(\text{Fe}^{2+} + \text{Mg}^{2+})$ on the individual sites. Figures 7, a, b, c, and d show the activity-composition relations in orthopyroxene (Fe, Mg) SiO_3 at various temperatures. It is assumed that the silicate framework does not change significantly and its contribution to the change in activity with temperature may be neglected. Therefore $a_{\text{Fe}}^{\text{Opx}}$ is similar to $a_{\text{FeSiO}_3}^{\text{Opx}}$ in these results. Table 4 shows the activity-composition data at different temperatures. The relations presented in these figures obey the Gibbs-Duhem equation:

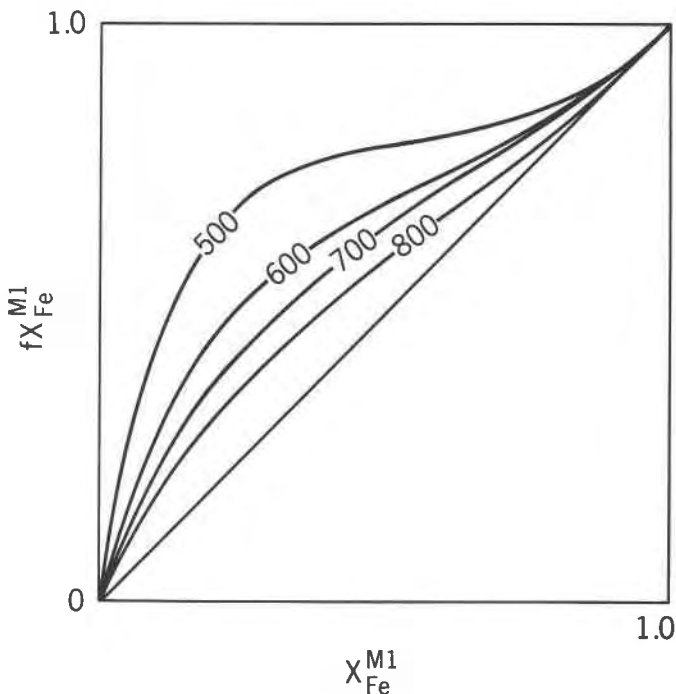


FIG. 5. Partial activity-composition relation for the $M1$ site.

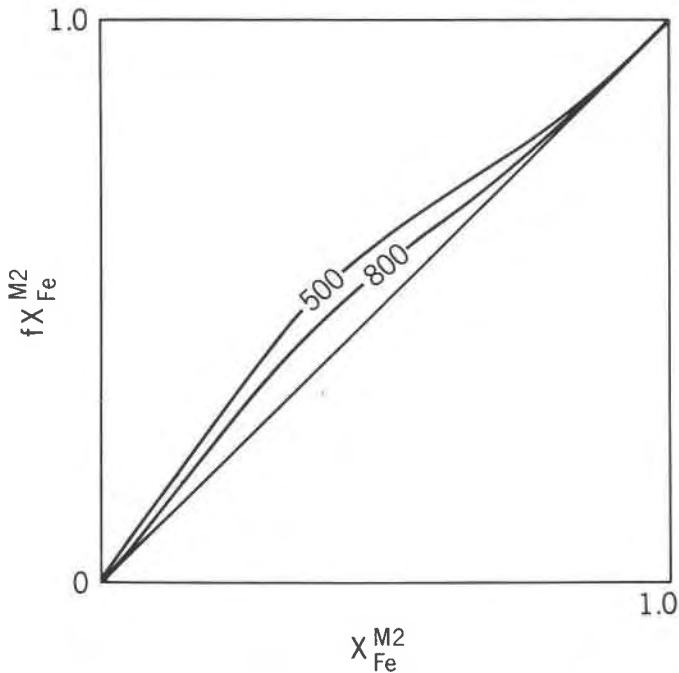


FIG. 6. Partial activity-composition relation for the M_2 site.

$$\left(X_{\text{Fe}} \frac{\partial \ln f_{\text{Fe}}}{\partial X_{\text{Fe}}} + X_{\text{Mg}} \frac{\partial \ln f_{\text{Mg}}}{\partial X_{\text{Fe}}} \right)_{PT} = 0 \quad (12)$$

ANALYTICAL EXPRESSIONS FOR THE ACTIVITY-COEFFICIENTS

It is convenient to express the activity coefficients as a polynomial in $X_{\text{Fe}}^{\text{OPX}}$. The following Redlich and Kister equations (see King, 1969) are used for this purpose:

$$\log f_{\text{Fe}} = X_{\text{Mg}}^2 \{ B + C(3X_{\text{Fe}} - X_{\text{Mg}}) + D(X_{\text{Fe}} - X_{\text{Mg}})(5X_{\text{Fe}} - X_{\text{Mg}}) \} \quad (13)$$

$$\log f_{\text{Mg}} = X_{\text{Fe}}^2 \{ B - C(3X_{\text{Mg}} - X_{\text{Fe}}) + D(X_{\text{Mg}} - X_{\text{Fe}})(5X_{\text{Mg}} - X_{\text{Fe}}) \} \quad (14)$$

A least squares curve is fitted to the data on activity coefficients at each temperature using the equation:

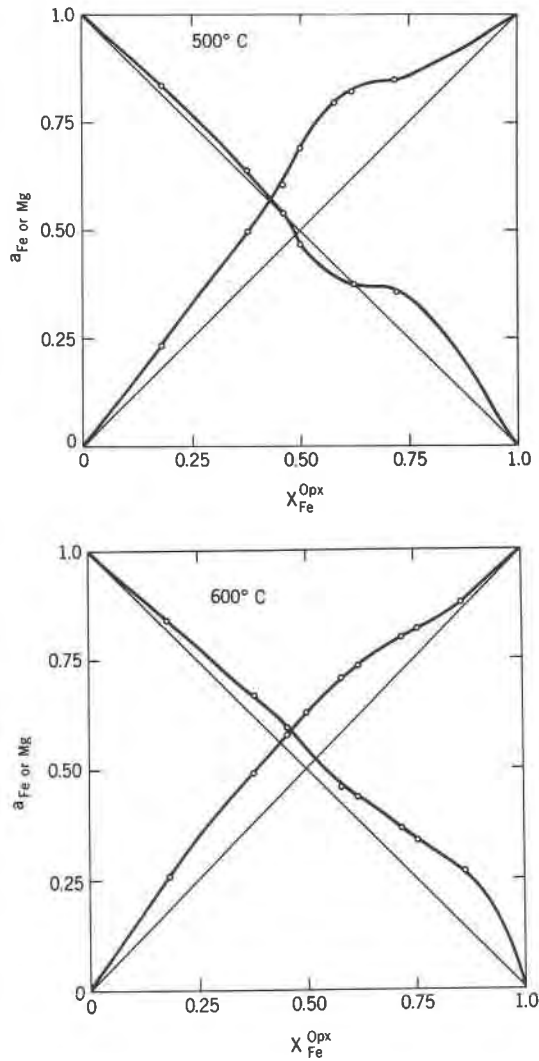


FIG. 7. Activity-composition relation in orthopyroxene, $(\text{Mg}, \text{Fe})\text{SiO}_3$ at 500, 600, 700, and 800°C. Smooth lines are drawn through the points.

$$\log \left(\frac{f_{\text{Fe}}}{f_{\text{Mg}}} \right) = B(X_{\text{Fe}} - X_{\text{Mg}}) + C(6X_{\text{Fe}}X_{\text{Mg}} - 1) + D(X_{\text{Fe}} - X_{\text{Mg}})(1 - 8X_{\text{Fe}}X_{\text{Mg}}) \quad (15)$$

The values of B , C and D are listed in Table 5.

Figure 8 shows the plots of $\log f$ against X_{Fe} . The curves are based on

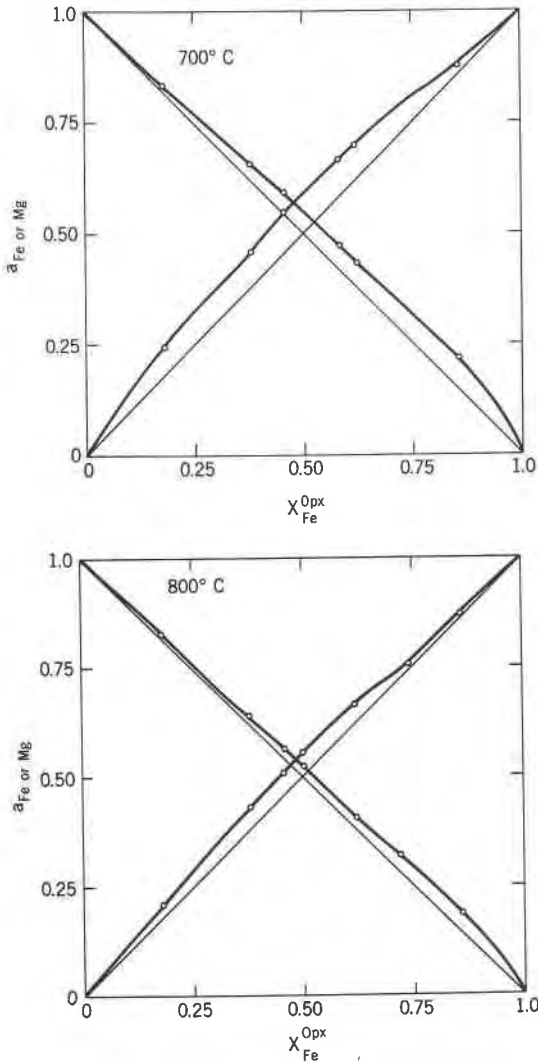


FIG. 7.—(Continued)

the expressions (13) and (14) and represent the experimental data well, except for those of the 500°C.

EXCESS THERMODYNAMIC FUNCTIONS

Guggenheim (1937) expressed the excess free energy of mixing, G^E for a binary system as:

$$G^E = X_A X_B \{ A_0 + A_1(X_A - X_B) + A_2(X_A - X_B)^2 + \dots \} \quad (16)$$

TABLE 4. ACTIVITY-COMPOSITION DATA ON ORTHOPYROXENE, (Mg, Fe)SiO₃

$X_{\text{Fe}}^{\text{Opx}}$	500°C	600°C	700°C	800°C
	a_{Fe}			
0.181	0.23	0.28	0.24	0.22
0.381	0.48	0.51	0.46	0.43
0.455	0.59	0.60	0.55	0.51
0.500	0.67	0.64	—	0.56
0.580	0.77	0.72	0.67	—
0.620	0.81	0.75	0.70	0.67
0.720	0.84	0.80	—	0.76
0.760	—	0.82	—	—
0.860	—	0.88	0.88	0.87
$X_{\text{Mg}}^{\text{Opx}}$	a_{Mg}			
	0.819	0.84	0.85	0.84
0.619	0.64	0.69	0.66	0.64
0.545	0.55	0.61	0.59	0.57
0.500	0.48	0.56	—	0.53
0.420	0.40	0.48	0.47	—
0.380	0.38	0.46	0.43	0.40
0.270	0.36	0.38	—	0.32
0.240	—	0.36	—	—
0.140	—	0.29	0.22	0.19

where A_0 , A_1 and A_2 are related to B , C , and D as $A_0 = 2.303 RTB$, $A_1 = 2.303 RTC$, and $A_2 = 2.303 RTD$ respectively. The values of A_0 , A_1 and A_2 are listed in Table 5.

Figure 9 shows a plot of G^E against X_{Fe} at various temperatures. Note that G^E may also be calculated from the experimental data by using the relation:

$$G^E = X_{\text{Fe}}RT \ln f_{\text{Fe}} + X_{\text{Mg}}RT \ln f_{\text{Mg}} \quad (17)$$

G^E calculated for the different samples using (17) differs somewhat depending upon the fit of the analytical expressions (13) and (14) to the data on individual isotherms as shown in Figure 8.

Excess entropy of mixing, S^E and excess enthalpy of mixing, H^E can be obtained by using the general thermodynamic formulae:

$$S^E = -RT \left(X_{\text{Fe}} \frac{\partial \ln f_{\text{Fe}}}{\partial T} + X_{\text{Mg}} \frac{\partial \ln f_{\text{Mg}}}{\partial T} \right) - R(X_{\text{Fe}} \ln f_{\text{Fe}} + X_{\text{Mg}} \ln f_{\text{Mg}}) \quad (18)$$

TABLE 5. VALUES OF THE CONSTANTS B , C , D , A_0 , A_1 AND A_2 FOR THE ANALYTICAL EXPRESSIONS FOR $\log f$ AND G^E

T°C	B	C	D	cal/mole		
				A_0	A_1	A_2
500	.260	.300	.250	919	1061	884
600	.280	.118	.190	1118	469	759
700	.212	.060	.130	944	267	579
800	.133	.048	.067	651	236	329

Note: The three constants are determined by fitting least squares curves to the activity-coefficient-composition data using analytical expressions (13, 14, and 15). The fitted curves are shown in Figure 8. A direct estimation of errors in these constants is difficult. The error in the calculation of log of activity coefficients is estimated to be ± 3 percent based on the errors in W^{M1} and W^{M2} listed in Table 3. The reliability of the A_0 value at 500°C is low (see p. 544).

$$H^E = -RT^2 \left(X_{\text{Fe}} \frac{\partial \ln f_{\text{Fe}}}{\partial T} + X_{\text{Mg}} \frac{\partial \ln f_{\text{Mg}}}{\partial T} \right) \quad (19)$$

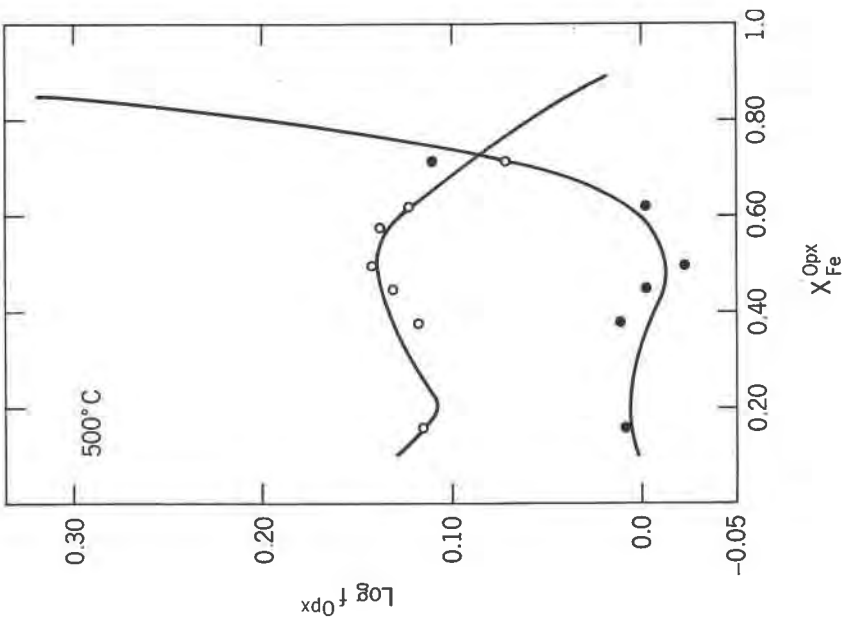
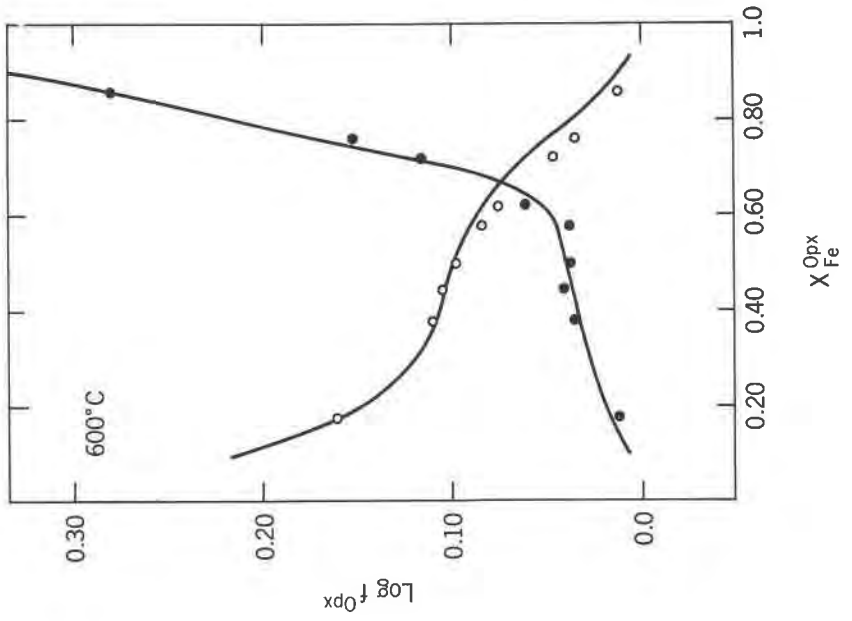
GENERAL CHARACTER OF THE ORTHOPYROXENE (Mg, Fe)SiO₃ CRYSTALLINE SOLUTION

The Asymmetric Solution. The activity-composition diagrams (Figures 7, a to d) and the plot of G^E against X_{Fe} in Figure 9 show that the orthopyroxene solution is asymmetric. The asymmetry increases with decreasing temperature. This relation can be examined quantitatively by studying the parameters A_0 , A_1 , and A_2 as a function of temperature. The expression for G^E is:

$$G^E = X_{\text{Fe}} X_{\text{Mg}} \{ A_0 + A_1(X_{\text{Fe}} - X_{\text{Mg}}) + A_2(X_{\text{Fe}} - X_{\text{Mg}})^2 \} \quad (20)$$

When the odd terms in the above expression vanish, the solution becomes symmetric. If A_2 and other higher terms are also zero, we obtain the model of simple mixture or the "regular" solution with A_0 as the "interchange energy" W . The asymmetry in the crystalline solution is then directly a function of the parameter A_1 .

Figure 10 shows a plot of A_0 , A_1 , and A_2 against temperature. A_0 decreases systematically with temperature in the range of 600 to 800°C. A_1 and A_2 vary regularly in the entire range of experimental temperatures. The trend of variation for A_1 indicates that the asymmetry in the solution increases very rapidly with decreasing temperature. On the other hand, with increasing temperature A_1 approaches a constant value of approximately 200 cal/mole. This means that even when A_0 and A_2



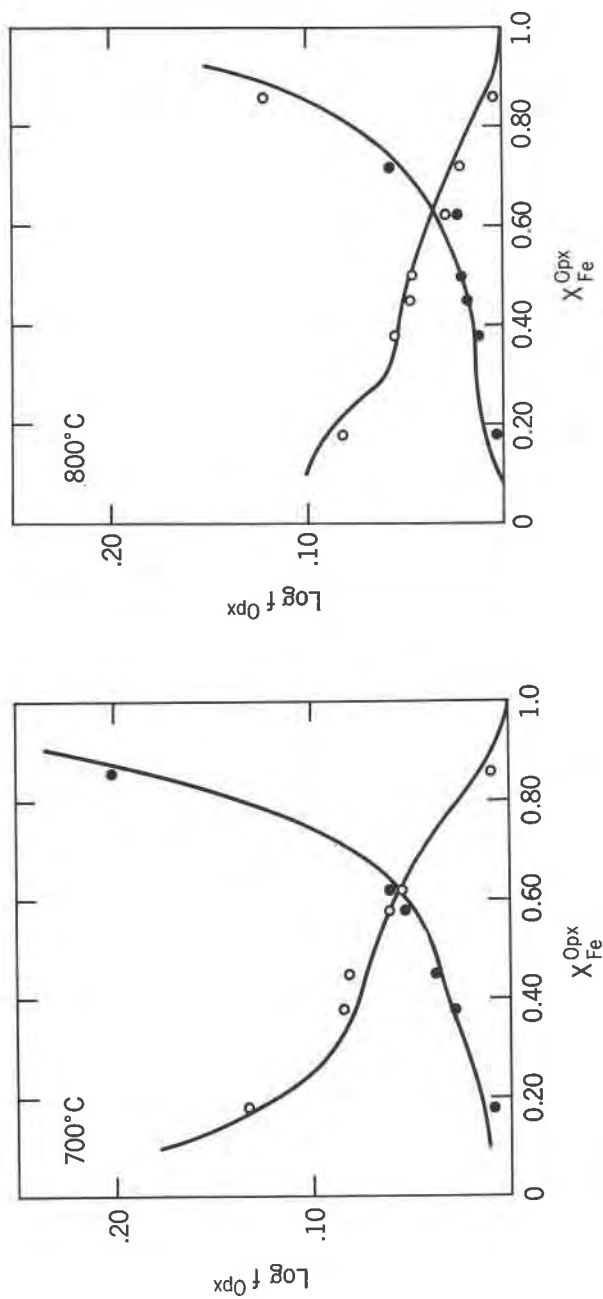


FIG. 8. Plots of $\log f$ against X_{Fe}^{Opx} at 500, 600, 700 and 800°C. Open circles- $\log f_{Mg}$. Filled circles- $\log f_{Fe}$. The least squares curves are based on the analytical expression with three constants B , C and D due to Redlich and Kister (King, 1969).

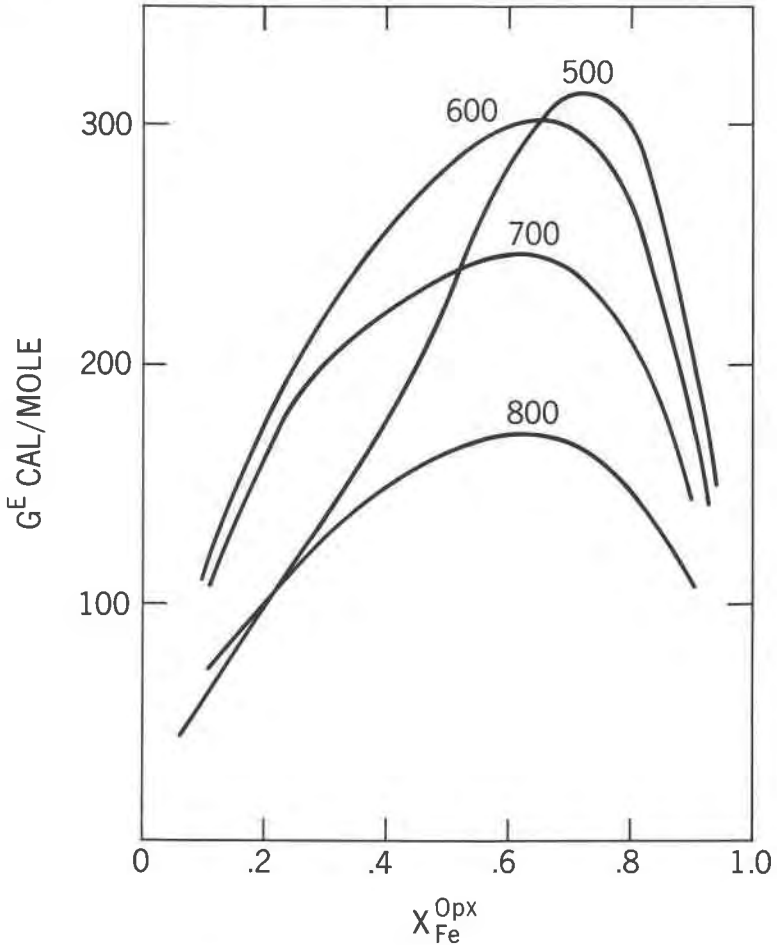


FIG. 9. Plot of the excess free energy G^E obtained by using Guggenheim's (1937) expression with three constants A_0 , A_1 and A_2 . These constants are calculated from the three constants B , C and D and are listed in Table 5.

become zero (approximately at 900°C), that is, when the solution is nearly ideal, some asymmetry would still persist. Note that in the present case, a positive value of A_1 means that higher values of G^E of mixing are associated with the Fe rich side.

Free Energy of Mixing and Critical Temperature. The activity-composition diagram at 500°C shows a tendency for the curve to flatten as X_{Fe} approaches 0.70. This is related to the asymmetry of the solution.

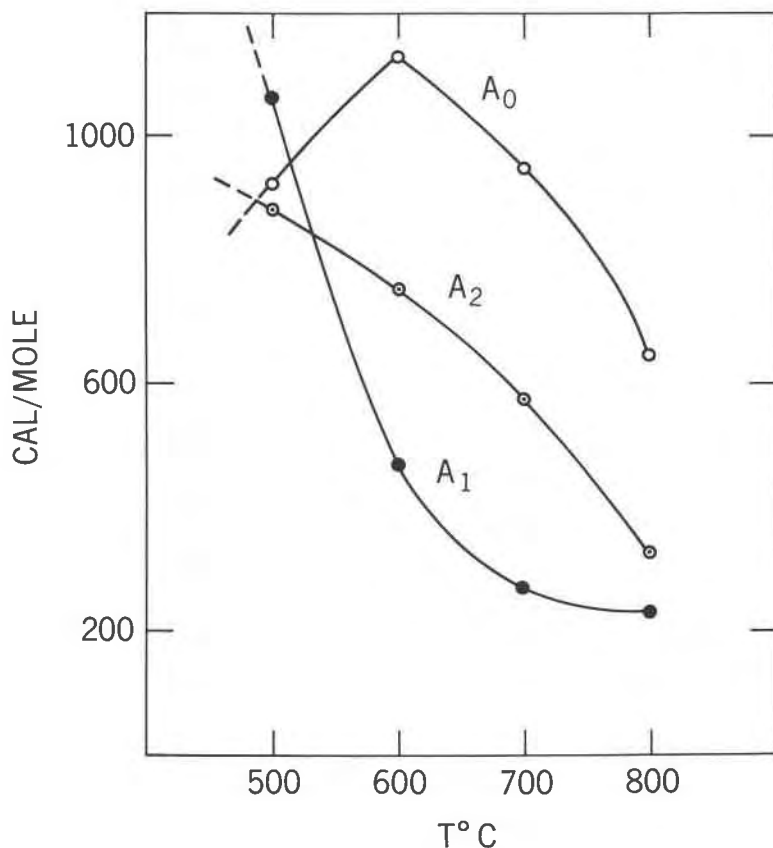


FIG. 10. Plot of three constants A_0 , A_1 and A_2 in Guggenheim's (1937) expression for G^E against temperature.

It appears that if A_1 increases beyond a critical value, unmixing may occur in the solution. The critical temperature should lie between 400 and 500°C. Combining the analytical expression (17) for G^E with the formulae for free energy of mixing for ideal solutions, the total free energy of mixing G^M may be calculated from the relation:

$$G^M = G^E + RTX_{Fe} \ln X_{Fe} + RTX_{Mg} \ln X_{Mg} \quad (21)$$

The values of A_0 , A_1 , and A_2 at 400°C obtained by extrapolation are 680, 1500, and 980 cal/mole respectively. The values of G^M at various temperatures are plotted in Figure 11. The curves tend to straighten out in the Fe rich region, especially at lower temperatures. The curve at 400°C shows a compositional range ($X_{Fe}=0.75$ to 0.90) where the ortho-

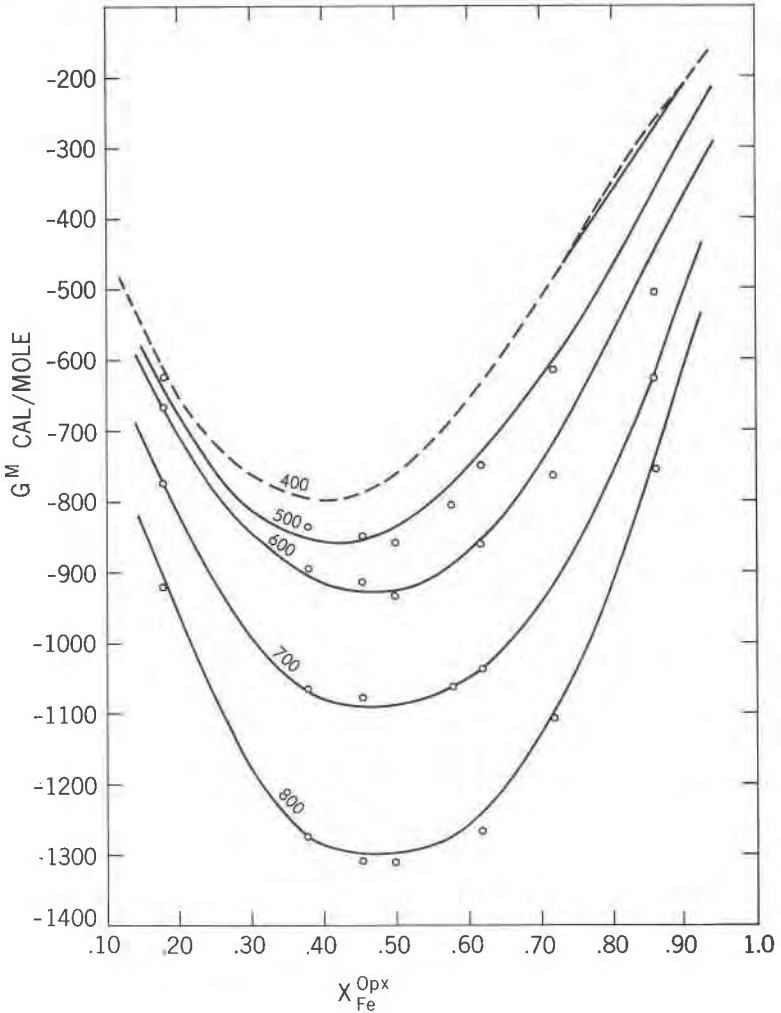


FIG. 11. Plot of the free energy of mixing G^M against X_{Fe} . The solid curves are drawn using Guggenheim's analytical expression for G^E . The open circles represent G^M for the samples calculated directly by using the equation: $G^M = X_{Fe}RT \ln a_{Fe} + X_{Mg}RT \ln a_{Mg}$. The dashed curve is based on extrapolated values of A_0 , A_1 and A_2 to 400°C and shows that orthopyroxene with X_{Fe} between 0.75 to 0.90 would unmix into two co-existing pyroxenes.

pyroxene would unmix into two coexisting solutions, one somewhat richer in Fe than the other. The critical temperature, when unmixing begins, may be close to 500°C.

CONCLUSIONS

The experimental data on the distribution of Mg^{2+} - Fe^{2+} between $M1$ and $M2$ sites in orthopyroxenes heated at various temperatures as determined by the Mössbauer resonance technique were found to yield smooth distribution isotherms, which are in better agreement with distribution curves based on Guggenheim's "simple mixture" model than with the ideal solution model for the sites. The deviation from the ideal solution model increases with decrease in temperature. Mixing of Mg^{2+} and Fe^{2+} on the $M1$ site was found to be more non-ideal than that on the $M2$ site. The orthopyroxene crystalline solution as a whole is non-ideal (asymmetric) in the range of 500 to 800°C. The non-ideality decreases rapidly with increasing temperature. The Redlich and Kister equations for the activity composition relation and Guggenheim's expression for the excess free energy of mixing were found to be particularly useful in expressing the thermodynamic nature of the orthopyroxene solution.

ACKNOWLEDGMENTS

We are greatly indebted to Dr. P. Butler, Jr., Profs. H. Ramberg and T. F. W. Barth for donation of samples; W. R. Riffle for assistance with Mössbauer experiments; F. Wood for microprobe analysis, Dr. J. Weidner for help with the heating experiments; C. W. Kouns for mineral separation; and Mrs. C. Inman for the preparation of absorbers and microprobe mounts. Prof. S. S. Hafner helped initially in setting up the Mössbauer spectrometer. Dr. B. J. Evans kindly supplied the computer program for Mössbauer data reduction. Discussions with Drs. R. F. Mueller and L. S. Walter have been most fruitful.

REFERENCES

- BANCROFT, G. M., R. G. BURNS, AND R. A. HOWIE (1967) Determination of the cation distribution in the orthopyroxenes series by the Mössbauer effect. *Nature* **213**, 1221-1223.
- BANNO, S., AND Y. MATSUI (1966) Intracrystalline exchange equilibrium in orthopyroxene. *Proc. Japan Acad.* **42**, 629-633.
- (1967) Thermodynamic properties of intracrystalline exchange solid solution. *Proc. Japan Acad.* **43**, 762-767.
- BENCE, A. E., AND A. L. ALBEE (1968) Empirical correction factors for the electron micro-analysis of silicates and oxides. *J. Geol.* **76**, 382-403.
- BUTLER, P., JR. (1969) Mineral compositions and equilibria in the metamorphosed iron formation of the Gagnon region, Quebec, Canada. *J. Petrology* **10**, 56-101.
- DIENES, G. J. (1955) Kinetics of order-disorder transformations. *Acta Met.* **3**, 549-557.
- DUNDON, R. W., AND L. S. WALTER (1967) Ferrous ion order-disorder in meteoritic pyroxenes and the metamorphic history of chondrites. *Earth Planet. Sci. Lett.* **2**, 372-376.
- EVANS, B. J., S. GHOSE, AND S. HAFNER (1967) Hyperfine splitting of ^{57}Fe and Mg-Fe order-disorder in orthopyroxenes ($MgSiO_3$ - $FeSiO_3$ solid solution). *J. Geol.* **75**, 306-322.
- FOWLER, R., AND E. A. GUGGENHEIM (1939) *Statistical Thermodynamics*. University Press, Cambridge.

- GHOSE, S. (1961) The crystal structure of a cummingtonite. *Acta Crystallogr.* **14**, 622-627.
- (1965) Mg^{2+} - Fe^{2+} order in an orthopyroxene, $Mg_{0.98}Fe_{1.07}Si_2O_6$. *Z. Kristallogr.* **122**, 81-99.
- AND S. S. HAFNER (1967) Mg^{2+} - Fe^{2+} distribution in metamorphic and volcanic orthopyroxenes. *Z. Kristallogr.* **125**, 157-162.
- AND E. HELLNER (1959) The crystal structure of grunerite and observations on the Mg-Fe distribution. *J. Geol.* **67**, 691-701.
- GROVER, J. E., AND P. M. ORVILLE (1969) The partitioning of cations between co-existing single- and multi-site phases with application to the assemblages: orthopyroxene-clinopyroxene, and orthopyroxene-olivine. *Geochim. Cosmochim. Acta* **33**, 205-226.
- GUGGENHEIM, E. A. (1937) Theoretical basis of Raoult's law. *Trans. Faraday Soc.* **33**, 151-159.
- (1952) *Mixtures*. Clarendon Press, Oxford.
- (1967) *Thermodynamics*. North Holland Publishing Co. Amsterdam.
- KING, M. B. (1969) *Phase Equilibrium in Mixtures*. Pergamon Press, London.
- KITAYAMA, K., AND T. KATSURA (1968) Activity measurements in orthosilicate and meta-silicate solid solutions. I. Mg_2SiO_4 - Fe_2SiO_4 and $MgSiO_3$ - $FeSiO_3$ at 1204°C. *Chem. Soc. Jap. Bull.* **41**, 1146-1151.
- MARZOLF, J. G., J. T. DEHN, AND J. F. SALMON (1967) Mössbauer studies of tektites, pyroxenes, and olivines. *Adv. Chem. Ser.* **68**, 61-85.
- MATSUI, Y., AND S. BANNO (1965) Intracrystalline exchange equilibrium in silicate solid solutions. *Proc. Japan Acad.* **41**, 461-466.
- MUELLER, R. F. (1961) Analysis of relations among Mg, Fe, and Mn in certain metamorphic minerals. *Geochim. Cosmochim. Acta* **25**, 267-296.
- (1962) Energetics of certain silicate solid solutions. *Geochim. Cosmochim. Acta* **26**, 581-598.
- (1964) Theory of immiscibility in mineral systems. *Mineral. Mag.* **33**, 1015-1023.
- (1967) Model for order-disorder kinetics in certain quasi-binary crystals of continuously variable composition. *J. Phys. Chem. Solids* **28**, 2239-2243.
- (1969) Kinetics and thermodynamics of intracrystalline distributions. *Mineral. Soc. Amer. Spec. Pap.* **2**, 83-93.
- , S. GHOSE, AND S. K. SAXENA (1970), Partitioning of cations between coexisting single- and multi-site phases. A discussion. *Geochim. Cosmochim. Acta* **34**, 1356-1360.
- NAFZIGER, R. H., AND A. MUAN (1967) Equilibrium phase compositions and thermodynamic properties of olivines and pyroxenes in the system MgO - FeO - SiO_2 . *Amer. Mineral.* **52**, 1364-1385.
- RAMBERG, H. (1944) Petrologic significance of sub-solidus phase transformations in mixed crystals. *Norsk Geol. Tidsskr.* **24**, 42-74.
- (1952) *The Origin of Metamorphic and Metasomatic Rocks*. Univ. Chicago Press, Chicago.
- AND G. W. DEVORE (1951) The distribution of Fe^{2+} and Mg^{2+} in co-existing olivines and pyroxenes. *J. Geol.* **59**, 193-210.
- SAXENA, S. K. (1968), Chemical study of phase equilibria in charnockites, Varberg, Sweden. *Amer. Mineral.* **53**, 1674-1695.
- (1969) Silicate solid solution and geothermometry. Part 1. Use of the regular solution model. *Contr. Mineral. Petrology* **21**, 338-345.
- AND S. GHOSE (1970) Order-disorder and the activity-composition relation in a binary crystalline solution. Part 1. Metamorphic orthopyroxene. *Amer. Mineral.* **55**, 1219-1225.

- SHENOY, G. K., G. M. KALVIUS, AND S. S. HAFNER (1969) Magnetic behaviour of the FeSiO_3 - MgSiO_3 orthopyroxene system from NGR in ^{57}Fe . *J. Appl. Phys.* **40**, 1314-1316.
- THOMPSON, J. B., JR. (1969) Chemical reactions in crystals. *Amer. Mineral.* **54**, 341-375.
- (1970) Chemical reactions in crystals. Corrections and clarifications. *Amer. Mineral.* **55**, 528-538.
- VIRGO, D., AND S. S. HAFNER (1969) Fe^{2+} , Mg order-disorder in heated orthopyroxenes. *Mineral. Soc. Amer. Spec. Pap.* **2**, 67-81.
- (1970) Fe^{2+} , Mg order-disorder in natural orthopyroxenes. *Amer. Mineral.* **55**, 201-223.

Manuscript received, July 27, 1970; accepted for publication, October 31, 1970.